https://doi.org/10.5194/egusphere-2022-167
Preprint. Discussion started: 19 April 2022

Potential for bias in effective climate sensitivity from state-dependent energetic balance

Benjamin M. Sanderson[1] **and Maria Rugenstein**[2]

[1]CICERO, Oslo, Norway
[2]Colorado State University, Fort Collins CO, USA

Correspondence: Benjamin Sanderson (benjamin.sanderson@cicero.oslo.no)

Abstract. To estimate equilibrium climate sensitivity, a common approach is to linearly extrapolate temperatures as a function of top of atmosphere energetic imbalance ("Effective Climate Sensitivity"). In this study, we consider an alternative approach for estimating equilibrium climate sensitivity through Bayesian calibration of a multiple timescale simple climate model. Results suggest potential biases in effective sensitivity estimates in the case of particular models where radiative tendencies imply energetic imbalances which differ between pre-industrial and quadrupled CO_2 states. These biases imply the need for reconsideration of some model published values of climate sensitivity, and the presence of radiative imbalances in a number of CMIP5 and CMIP6 models underlines the urgent requirement for operational climate sensitivity experiments on millennial timescales to assess if such biases exist in estimates of climate sensitivity in the wider CMIP ensembles.

1 Introduction

Equilibrium Climate Sensitivity (*ECS*) of an Earth System Model is the equilibrium increase in global mean temperature experienced in response to an instantaneous doubling in carbon dioxide concentrations over pre-industrial levels. Introduced as a metric of response of the Earth System to greenhouse gases in the early years of computational climate science (Charney et al., 1979; Hansen et al., 1984), it remains a very common metric of the sensitivity of the Earth to greenhouse gas forcing (Knutti et al., 2017; Masson-Delmotte et al., 2021).

Measuring *ECS* in a coupled climate model, however, is difficult owing to the time required for the equilibration of the system to a change in forcing (Wetherald et al., 2001; Solomon et al., 2010; Jarvis and Li, 2011) necessitating simulations of multiple millennia to obtain a near-equilibrated estimate of temperature response (Rugenstein et al., 2020). The computational burden of conducting such simulations implies that standard practise for model assessment is to measure an "Effective Climate Sensitivity" (*EffCS*) using feedbacks extrapolated from those simulated in the first 150 years simulation forced with a step-wise quadrupling of CO_2 (Gregory et al., 2004; Murphy, 1995; IPCC, 2013; Forster, 2016; Andrews et al., 2012).

A core assumption in the calculation of *EffCS* is that the system will ultimately stabilise in a state of energetic balance (Gregory et al., 2004). However, in practise a number of models exhibit energetic radiative top of atmosphere imbalances in the control state in both CMIP5 (Hobbs et al., 2016) and CMIP6 (Irving et al., 2021), and as such the Effective Climate Sensitivity is calculated using net flux anomalies relative to the control mean top of atmosphere net radiative fluxes. However, it remains untested as to whether such models will ultimately converge to the same state of imbalance.

In the present study, we consider an alternative approach for calculating climate sensitivity from a climate simulation in which there is a step change in carbon dioxide concentrations. We consider how the method of calculating effective climate sensitivity, either from initial response or from millennial scale simulations, may be potentially subject to biases arising from assumptions on the equilibrated radiative state. Finally, we consider how these uncertainties relate to our confidence in the relationship between transient and equilibrium climate feedbacks.

https://doi.org/10.5194/egusphere-2022-167
Preprint. Discussion started: 19 April 2022

We consider the role of non-equilibrated models in the context of recent research, which has highlighted potential uncertainties in the *EffCS* approximation of *ECS* - studies have found that net radiative feedbacks can exhibit both timescale and state dependencies (e.g.Senior and Mitchell 2000; Armour et al. 2013; Andrews et al. 2015; Rugenstein et al. 2016; Proistosescu and Huybers 2017; Pfister and Stocker 2017; Dunne et al. 2020; Andrews et al. 2018; Bloch-Johnson et al. 2021) both of which draw into question the implicit constant feedback assumption used to calculate *EffCS*.

The LongrunMIP project set out in part to quantify this error by running a subset of ESMs in idealised carbon dioxide perturbation experiments with simulations of millennial timescale response (Rugenstein et al., 2019). Initial studies compared the *EffCS* as derived using the first 150 years of the simulation with that derived using the last 15 percent of warming in multi-thousand year experiments - finding that the accuracy of the *EffCS* varied by model, but the two methods differed by 5-37% or less in the estimate of *ECS* (Rugenstein et al., 2020). A follow-up study (Rugenstein and Armour, 2021) considered a range of approaches for characterising feedbacks on different timescales, and found that feedbacks assessed in the period 100-400 years after the initial quadrupling of CO_2 concentrations may provide a practical prediction of equilibrium response accurate within 5% or less. They found also, however, there were large inconsistencies in some models between estimates of climate sensitivity derived from extrapolation to radiative equilibrium and those methods which relied on a fitting of exponentially decaying temperature trend, leaving uncertainty on the best practise for integrating model-derived *EffCS* distributions into uncertainty in long term warming trajectories.

A general assessment of the likely range of *EffCS* (Sherwood et al., 2020) explicitly requires prior assumptions on the ratio of *ECS*:*EffCS* (represented by their parameter ζ such that *ECS*/*EffCS* is given by $(1+\zeta)$). The confidence in the upper bound of *EffCS* rested strongly on combined historical and paleo evidence, which together implied that ζ is small, contributing to the headline result that values of *EffCS* of greater than 4.7K are unlikely. These findings somewhat challenge the use of the CMIP6 ensemble of climate models as a proxy for climate projection uncertainty in assessment, given approximately 1/3 of the ensemble have *EffCS* values of greater than 4.7K (O'Neill et al., 2016; Eyring et al., 2016; Meehl et al., 2020). The high *EffCS* values in CMIP6 are in most models due to less negative cloud feedbacks than in CMIP5 (Zelinka et al., 2020).

So how plausible are the higher sensitivity models? Studies have found that one of the higher sensitivity models (CESM2) tend to perform more poorly in paleoclimate simulations than its lower sensitivity predecessors (Zhu et al., 2020). Although studies suggest that post-1980 warming may help constrain the Transient Climate Response (Jiménez-de-la Cuesta and Mauritsen, 2019; Nijsse et al., 2020; Tokarska et al., 2020), recent historical warming alone is more weakly correlated with *EffCS* in the CMIP5 ensemble (Tokarska and Gillett, 2018), consistent with the fact that a given value of TCR can be achieved with a wide range of thermal response timescales and amplitudes (Sanderson, 2020; Sherwood et al., 2020).

2 Methods

We consider available pre-industrial control simulations (*PICTRL*) and abrupt CO_2 quadrupling experiments (*ABRUPT4X*) from three available ensembles: CMIP5 (Taylor et al., 2012), CMIP6 (Eyring et al., 2016) and LongRunMIP (Rugenstein et al., 2019).

For LongrunMIP simulations, we use *ABRUPT4X* simulations where available, but for models which have run alternative long term extensions, we scale them accordingly, combining with available 150 year *ABRUPT4X* simulations to produce a composite estimate of long term response to CO_2 quadrupling (see Appendix). For each simulation, we compute global averages of surface temperature, and top of atmosphere shortwave and longwave fluxes.

We assume that the temperature and radiative timeseries can be modelled by a sum of exponential decay terms, a basis set which is consistent with the general solution of two layer simple climate models (with or without terms for ocean heat uptake efficacy) (Caldeira and Myhrvold, 2013; Proistosescu and Huybers, 2017; Sanderson, 2020; Geoffroy et al., 2013a; Winton et al., 2010; Smith et al., 2018; Geoffroy et al., 2013b)

As in Proistosescu and Huybers (2017), we allow for three independent equilibration timescales, such that:

$$T(t) = \sum_{n=1}^{3} S_n(1 - e^{-(t/\tau_n)}) + T_0 \tag{1a}$$

$$R(t) = \sum_{n=1}^{3} R_n(1 - e^{-(t/\tau_n)}) + R^{4x} \tag{1b}$$

Where $T(t)$ and $R(t)$ are the global annual mean surface temperature and net top of atmosphere radiative flux timeseries respectively, τ_n is the decay time associated with the timescale n, S_n and R_n are scaling factors and T_0 and R^{4x} are constant terms. T_0 is taken as the mean temperature in the last available 500 years of the control simulation (if fewer than 500 *PICTRL*

https://doi.org/10.5194/egusphere-2022-167
Preprint. Discussion started: 19 April 2022

Parameter	long name	Units	Min value	Max value
S_1	Short timescale sensitivity	K	0	10
S_2	Intermediate timescale sensitivity	K	0	10
S_3	Long timescale sensitivity	K	0	10
T_0	Control mean temperature	K	n/a	n/a
τ_1	Short timescale	years	0	10
τ_2	Intermediate timescale	years	10	150
τ_3	Long timescale	years	150	2000
R_0	Equilibrium energy leak (*PICTRL*)	Wm^{-2}	-5	5

Table 1. Parameters and prior ranges considered in the Bayesian calibration of Eq. 1a.

years are available, all available years are used). R_0^{4x} represents the radiative flux imbalance at $t = 0$ and is calibrated during the calculation.

We assess the radiative imbalance in the control simulation, R_0^{CTRL}, as the time average of net Top of Atmosphere (TOA) flux from the last 100 years of *PICTRL*. In fully equilibrated models with no energetic leaks, it would be expected that $R^{CTRL} = 0$, but it has been noted previously that this is not always the case and small energetic imbalances remain in some models even after the model global mean temperature trends have ceased (Rugenstein et al., 2019).

2.1 Bayesian Calibration of long term response parameters

We fit the response equations detailed in Eq. 1a to the output of each ensemble member's global mean radiative flux and surface temperature timeseries using a Markov Chain Monte Carlo optimizer (Foreman-Mackey et al. 2013; as implemented in the 'lmfit' Python module), allowing for $n = 3$ representative decay timescales. Parameter ranges are constrained according to Table 1.

The conventional effective climate sensitivity (*EffCS*) is calculated using the first 150 years of simulation. Control global mean temperatures and TOA energetic imbalances are expressed as anomalies relative to T_0. A second estimate of equilibrium warming, $\Delta T_{best-est}$, follows Rugenstein et al. (2020), by calculating the effective climate sensitivity based on the years corresponding to the last 15% of warming in the simulation (that is, for all years following the point when the simulation first exceeds 85% of the average global mean temperature anomaly in the last 20 years of the *ABRUPT4X* simulation).

We finally calculate a third estimate of climate sensitivity ΔT_{extrap} as in Eq. 2 in the equilibrated (*ABRUPT4X*) simulation using the ensemble of fitted parameters from Bayesian calibration of Equation 1a, using again global mean temperature anomalies from *ABRUPT4X* relative to T_0 (taken as mean temperatures over the last 100 years of *PICTRL*).

$$T_{extrap} = \sum_{n=1}^{3} S_n + T_0 \tag{2}$$

We estimate the long term radiative imbalance in the *ABRUPT4X* simulation from the fitted values for R^{4x} (the initial forcing at $t = 0$ in *ABRUPT4X*) and R_n (the amplitude of the decay in forcing at the timescale corresponding to τ_n) from Eq. 1b.

$$R_{extrap}^{4x} = \sum_{n=1}^{3} R_n + R^{4x}, \tag{3}$$

where R_{extrap}^{4x} is the estimate of long term radiative imbalance in the *ABRUPT4X* simulation. For models in which R_0^{CTRL} is itself non-zero, previous studies have assumed in the calculation of $\Delta T_{best-est}$ that this imbalance is a constant feature of the model (Rugenstein et al., 2020). Here, we explicitly predict the imbalance for long timescales where $t >> \tau_n$ for all n.

2.2 Results

The relationship between temperature and TOA fluxes for the fitted exponential models for *ABRUPT4X* simulations in the LongRunMIP archive are presented in Figure 1, while Figures 2 and 3 shows the temperature and TOA fluxes in isolation. Equilibrium warming ΔT_{extrap} and energetic imbalance R_{extrap}^{4x} are estimated from the all available data in CMIP5, CMIP6, and LongRunMIP (summarised in Figure 4). This estimate is subject to large errors in 150 year simulations in CMIP5 and CMIP6 (illustrated here by the 10th and 90th percentiles of the fitted range in the MCMC fitting process), but is relatively precise for the multi-millennial simulations in LongrunMIP (see Figure 2).

We note that there is significant model diversity in the behaviour of models in the approach to equilibrium, and in the consistency of different approaches. Some models (CESM104, MPIESM11 and MPIESM12) behave as expected, showing near-zero

https://doi.org/10.5194/egusphere-2022-167
Preprint. Discussion started: 19 April 2022

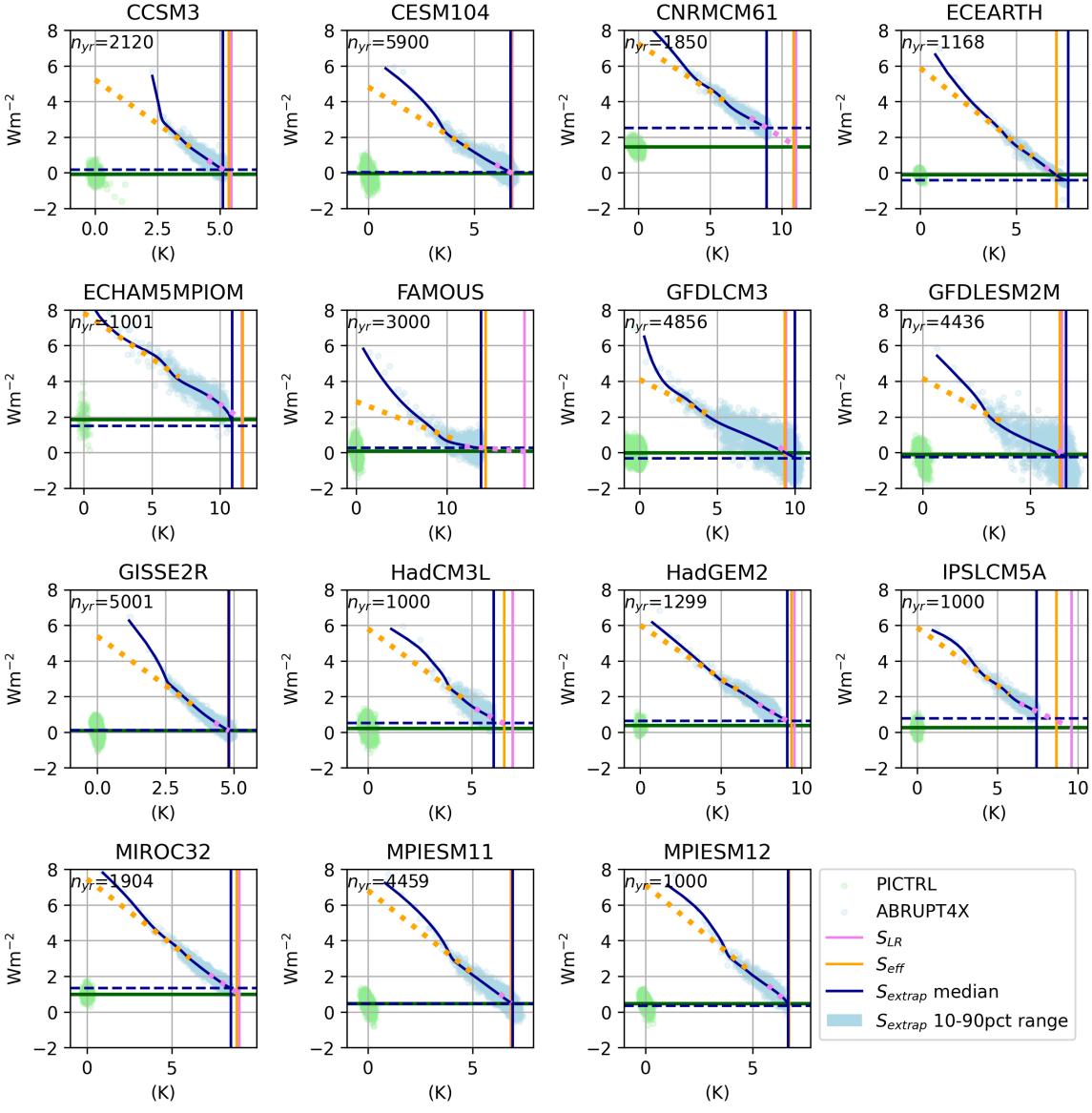

Figure 1. An illustration of global mean net radiative imbalance as a function of surface temperature for different members of the LongrunMIP archive. Vertical axis shows absolute top of atmosphere net radiative imbalance, horizontal axis shows surface temperature relative to the final 500 years of the control simulation. Blue points are individual years from *ABRUPT4X*. Yellow solid horizontal line show the *PICTRL* net energy imbalance averaged over the final 100 years of the simulation. Solid yellow and pink lines show linear regressions used to estimate effective climate sensitivity using the first 150 years of data (yellow) and the last 15% of warming (pink), vertical dotted pink and yellow lines show corresponding values of effective climate sensitivity. Dashed blue lines show the maximum likelihood exponential model fit using all available years in the simulation, while light blue ellipse shows the 5-95 confidence intervals for the corresponding values of ΔT_{extrap}

https://doi.org/10.5194/egusphere-2022-167
Preprint. Discussion started: 19 April 2022

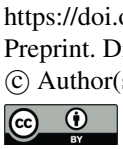

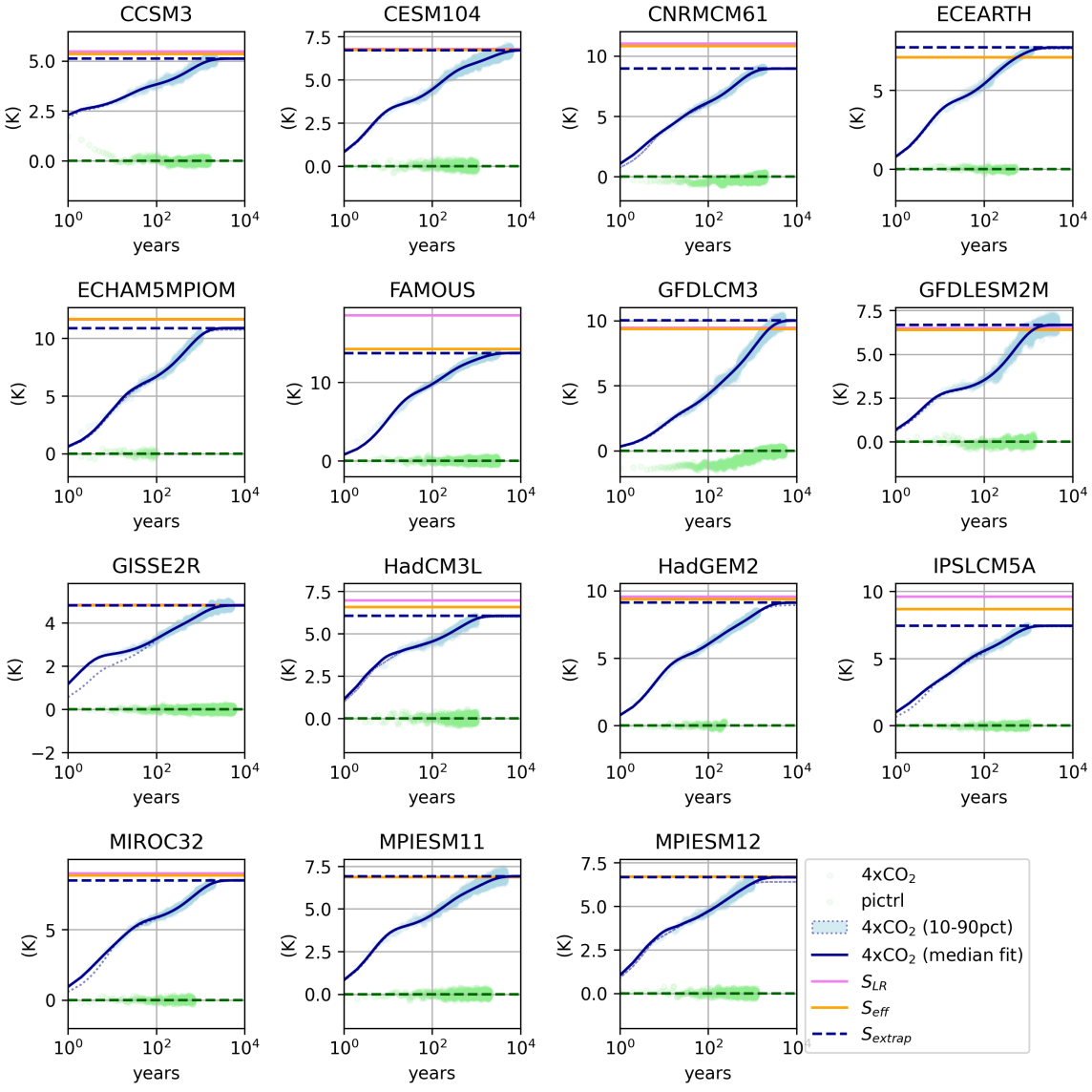

Figure 2. Global mean temperature anomaly with respect to the last 500 available years of the *PICTRL* simulation, plotted as a function of time (log scale) for the members of the LongrunMIP ensemble. Black points show annual global mean surface temperature anomalies from the *ABRUPT4X* simulation. Thick blue lines show the median top of atmosphere timeseries using the ensemble of three timescale exponential models from the posterior fitted distribution (see Section 2). Shaded regions and thin dotted lines show the 10th and 90th percentiles the fitted ensemble projections. Dashed horizontal line illustrates ΔT_{extrap}, yellow is $EffCS$ and purple is $\Delta T_{best-est}$.

https://doi.org/10.5194/egusphere-2022-167
Preprint. Discussion started: 19 April 2022

equilibrium TOA balance in both *PICTRL* and in the extrapolated *ABRUPT4X* simulation (Figure 3). In these simulations, $\Delta T_{best-est}$ and ΔT_{extrap} are nearly identical.

However, many models show significant differences in sensitivities estimated with the differing approaches (Figure 4). CNRMCM61, MIROC32 and IPSLCM5A have non-zero equilibrium TOA energetic balance, both in *PICTRL* and *ABRUPT4X* simulations, but there are significant differences between the equilibrium energetic imbalance in *PICTRL* and *ABRUPT4X* (Figure 3), which biases both $\Delta T_{best-est}$ and *EffCS*. For example, CNRMCM61 exhibits relatively constant feedbacks on century and millennial timescales, so $\Delta T_{best-est}$ and *EffCS* are similar (5.62K, 5.52K respectively), but ΔT_{extrap}, which is well fitted by the data is significantly lower (4.56±0.01K), see Figure 2) due to the differing estimated equilibrium energetic imbalance in *ABRUPT4X* and *PICTRL* simulations.

Other models (HadCM3L, FAMOUS, GFDLESM2M, GFDLCM3, ECEARTH) appear to show a control simulation in near energetic balance, but an *ABRUPT4X* simulation which converges to a state of energetic imbalance (Figure 3). This, in turn introduces a source of potential bias in the estimate of effective climate sensitivity if the system is converging to a non-equilibrated state - implying that the control simulation may be tuned to exhibit energetic balance but the equilibrated 4xCO_2 state is subject to an energy leak. A particularly extreme example is FAMOUS, where the small difference in extrapolated energetic balance, combined with strong curvature in the relationship between TOA fluxes and surface warming results in a much larger values of $\Delta T_{best-est}$ (9.27K) than ΔT_{extrap} (6.87K, see Table A2) or $EffCS$ (7.13K) (using $R^{4x}_{extrap} = -0.16Wm^{-2}$ rather than $R^{CTRL}_0 = -.01Wm^{-2}$ would result in a value of $\Delta T_{best-est} = 7.01K$, broadly consistent with $EffCS$ and ΔT_{extrap}). Similarly for HadCM3L, the fitted extrapolated sensitivity ΔT_{extrap} (3.03K, see Table A2) indicates a lower climate sensitivity than implied by $\Delta T_{best-est}$ (3.49K) and $EffCS$ (3.29K).

Looking at the wider CMIP5 and CMIP6 ensembles, it is apparent that a large number of models may be potentially subject to these biases, given that large flux imbalances are present in the control state (Figure 4). However, the standard CMIP5 and CMIP6 simulations contain insufficient data to fully assess ΔT_{extrap} (orR^{4x}_{extrap}) using the 3-mode fitting approach (see Figure 4), though in most cases the uncertainties in the fitted solution generally allow for equilibrium values which are higher then the effective climate sensitivity as assessed over the first 150 years of simulation. Only a small number of models allow for fitted solutions which have a lower ΔT_{extrap} than the *EffCS* (MIROC5, CNRMESM2.1, ACCESS-CM2). One of these cases (CNRMCM6.1) is a close relative of the CNRMESM2.1 - the LongrunMIP simulation which we identified to be potentially subject to biases owing to energetic imbalances in the 4xCO_2 equilibrium state.

3 Conclusions

We have considered an alternative approach for calculating long term tendencies of temperature and planetary energetic imbalance from simulations in which atmospheric carbon dioxide concentration is instantaneously perturbed. This approach relies on the assumption that the evolution of the system can be represented as a sum of decaying exponential terms with differing timescales. In order to produce confident results, the approach requires additional data beyond the conventional 150 years provided in CMIP climate simulation archives, however, an existing project, LongrunMIP, provides multi-millennial simulations which allow for a confident application of this approach.

We find that this approach highlights some potential limitations and biases associated with using effective climate sensitivity to predict equilibrium warming. It has been observed before that energetic imbalances exist in some models in the CMIP archive (Rugenstein et al., 2019; Hobbs et al., 2016; Irving et al., 2021), and in this study we show that such control state radiative imbalances are relatively widespread in CMIP5 and CMIP6.

The conventional assumption used to calculate effective climate sensitivity in these cases is that such imbalances remain constant, such that radiative anomalies from the control state can be used to calculate the effective climate sensitivity. Critically, in some LongrunMIP simulations, we observe that energetic imbalances exist both in the control state, and in the extrapolated tendencies of the simulations with CO_2 perturbations - but those imbalances are themselves state-dependent. This undermines the concept of effective climate sensitivity - if we do not know what the radiative imbalance will be when temperatures stabilise in an *ABRUPT4X* simulation, we in turn cannot predict the climate sensitivity with precision.

In practise, only some models in CMIP5 and CMIP6 appear to exhibit significant radiative imbalances in the control state (see Figure 4), and although the 150 year *ABRUPT4X* simulations are insufficient to assess if these energetic imbalances are state-dependent, these are the cases where we might be least confident in the effective climate sensitivity value. Models may exhibit non-equilibrium fluxes in the control state for a number of different reasons - either the model has not been run for sufficiently long in the control configuration to reach a state of energetic balance, or there is a persistent energetic leak in the model, which may be constant or evolving (Hobbs et al., 2016). In either case, the results presented in this study draw into doubt whether such imbalances can be assumed to remain constant in a climate perturbed through alteration of climate forcers.

https://doi.org/10.5194/egusphere-2022-167
Preprint. Discussion started: 19 April 2022

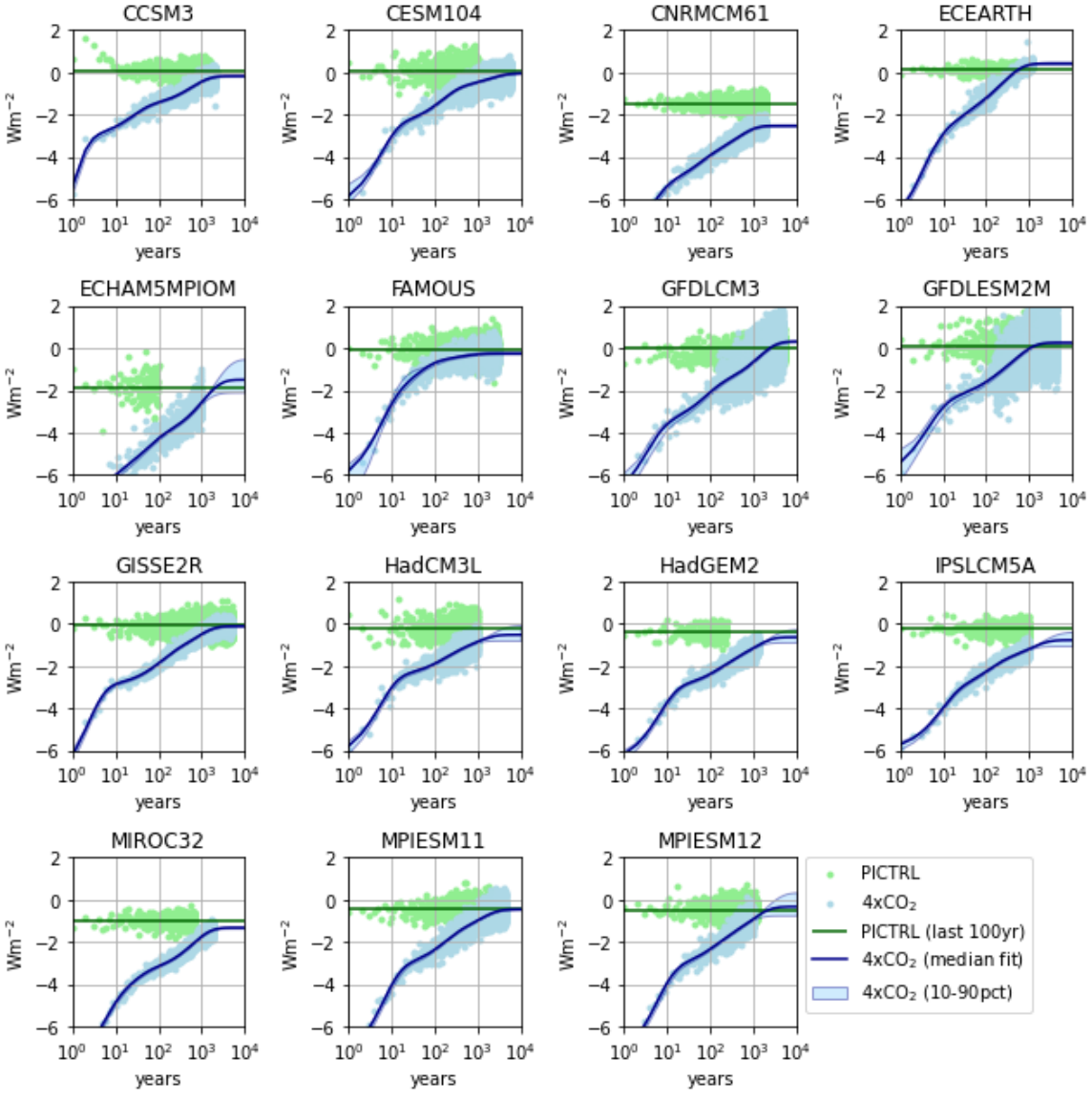

Figure 3. Top of atmosphere net radiative imbalance plotted as a function of time (log scale) for the members of the LongrunMIP ensemble. Semi-transparent blue and green points show annual mean upgoing net radiative flux from *PICTRL* and *ABRUPT4X*. Thick blue and green lines show the median TOA timeseries using the ensemble of 3 timescale exponential models from the posterior fitted MCMC distribution (see Section 2). Shaded regions and thin lines show the 10th and 90th percentiles the fitted ensemble projections.

https://doi.org/10.5194/egusphere-2022-167
Preprint. Discussion started: 19 April 2022

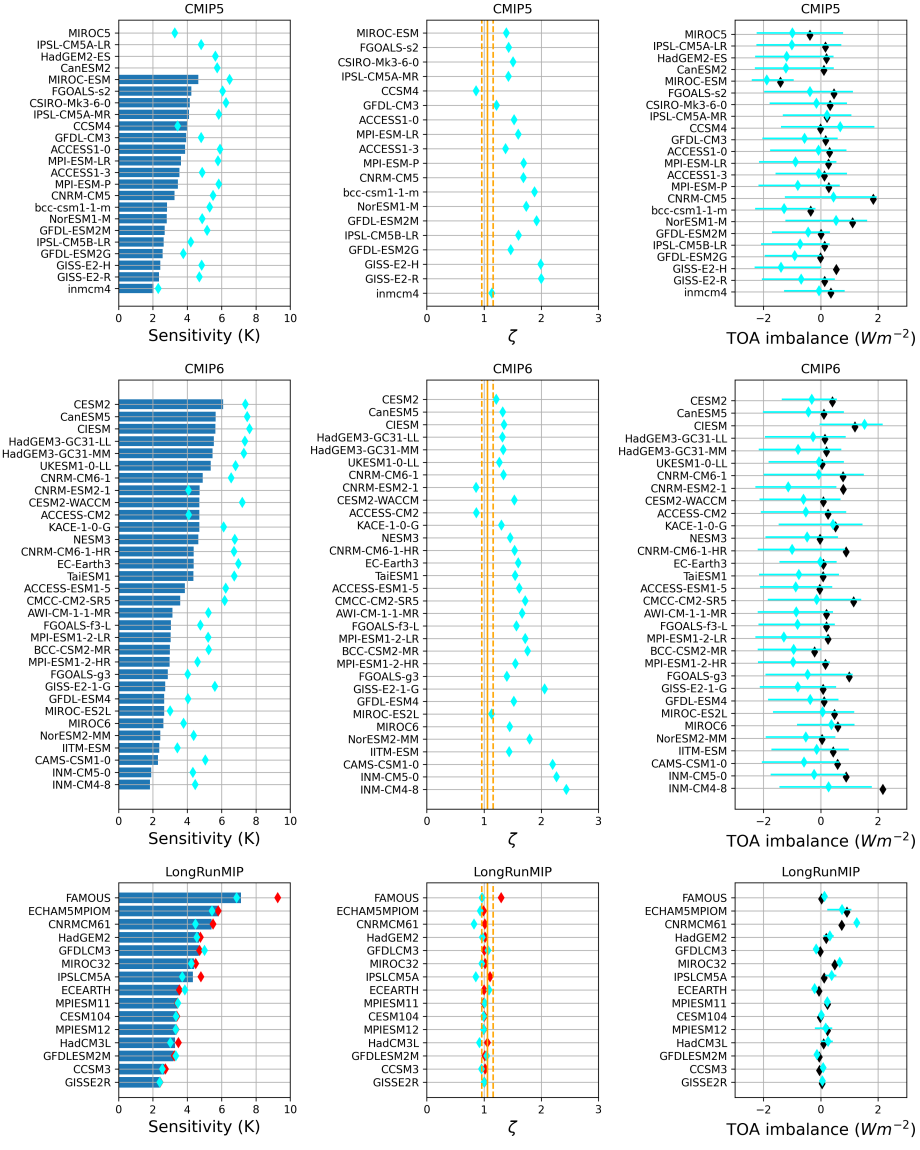

Figure 4. Barplots summarising results for three model ensembles, CMIP5 (top row), CMIP6 (middle row) and LongRunMIP (bottom row). Left hand column shows different estimates of equilibrium climate sensitivity. Solid blue bars show EffCS (see text). Light blue diamond and whiskers show the median, 10th and 90th percentiles $\Delta T_{\mathrm{extrap}}$ (fitted to all available years of the *ABRUPT4X* global mean temperature anomaly timeseries). For simulations of 500 years or longer, $\Delta T_{\mathrm{best-est}}$ (following Rugenstein et al. (2020)), is shown in red. The central column shows the ratio of estimated equilibrium climate sensitivity to effective climate sensitivity (ζ as defined in Sherwood et al. (2020)), as (1+$\Delta T_{\mathrm{extrap}}$)/EffCS (cyan errorbars) and $\Delta T_{best-est}$ using the the last 15% of warming (red diamonds). The right hand column shows R^{4x}_{extrap} (light blue diamond and whiskers) and R^{CTRL}_{0} (black diamonds).

https://doi.org/10.5194/egusphere-2022-167
Preprint. Discussion started: 19 April 2022

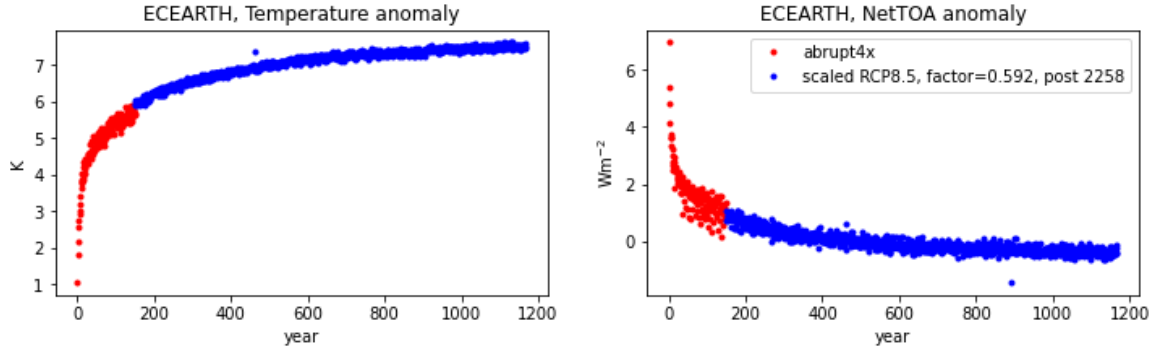

Figure A1. Illustration of composite *ABRUPT4X*CO_2 simulation for ECEARTH

Even models which are in or close to energetic balance in the control state fall into two potential categories: those where the energetic budget of the model is structurally closed through the elimination of all leaks, and those where the model parameters have been adjusted to produce near-zero net TOA fluxes in the control state. The latter case is still potentially subject to errors in the estimation of effective climate sensitivity, because if energetic imbalances are dependent on climate forcers, then the calibrated minimisation of net TOA fluxes may be inappropriate for the perturbed climate state. A simple analysis of the net fluxes in the control simulation cannot distinguish between structurally balanced models and tuned balanced models - but centers which operationally adjust parameters to minimize energetic losses should be aware of this potential bias in effective climate sensitivity.

Our results highlight the potential for error in the estimation of effective climate sensitivity through the assumptions on the asymptotic radiative balance of climate models. In the case of LongrunMIP - there is a significant difference between the distribution of fitted asymptotic values of energetic imbalance in *ABRUPT4X* compared with the mean energetic balance in *PICTRL* in 9 of 15 models (see Table A2). The potential for this bias in the wider CMIP ensembles, especially in cases where models are not equilibrated, highlights some of the concerns associated with energetic imbalances in the control simulations of some climate models, and the necessity of replicating the LongrunMIP approach as standard practise in CMIP in order to understand the robustness of our current model-derived assessments of uncertainty in the equilibrium response to climate forcers.

Appendix A: Treatment of Longrunmip data

LongrunMIP data is identical to that used in Rugenstein et al. (2020). Some models do not have multi-millennial simulations for *ABRUPT4X*CO_2 simulations. However, all LongrunMIP models have submitted at least one simulation exhibiting the long term response to a constant climate forcing. In these cases, we use the first 150 years from published *ABRUPT4X*CO_2 simulations, and scale simulations from other available contributions to estimate the multi-millennial response (see Table A1. Temperature and net Top of Atmosphere radiative anomalies are scaled by the ratio of the long term forcing used in the submitted experiment, and that corresponding to a quadrupling of carbon dioxide.

GFDL models (GFDLCM3 and GFDLESM2M) submit an extension to the 1pctCO_2 simulation, which keep CO_2 concentrations constant after year 70, at double pre-industrial levels. For these simulations, we scale anomalies by a factor of 2 (see Figures A2 and A3). MIROC32 submits an extension to 1pctCO_2 which branches in year 140, when CO_2 concentrations are quadrupled - hence anomalies are not scaled (see Figures A4). ECEARTH submits an extension to RCP8.5 - the forcing for which stabilizes post-2250 (Meinshausen et al., 2011), hence long term extensions are scaled by the ratio of estimated long term forcing in response to CO_2 quadrupling (7.4Wm^{-2}, Myhre et al. (2013)) and the RCP8.5 long term stable forcing value of 12.5Wm^{-2} (see Figures A1).

We seek to splice runs in year 145 of the abrupt 4xCO_2 simulation, and thus we determine a splicing point in the donor simulation where the top of atmosphere radiative imbalance is equal to the decadal average imbalance in years 141-150 of the *ABRUPT4X* simulation.

https://doi.org/10.5194/egusphere-2022-167
Preprint. Discussion started: 19 April 2022

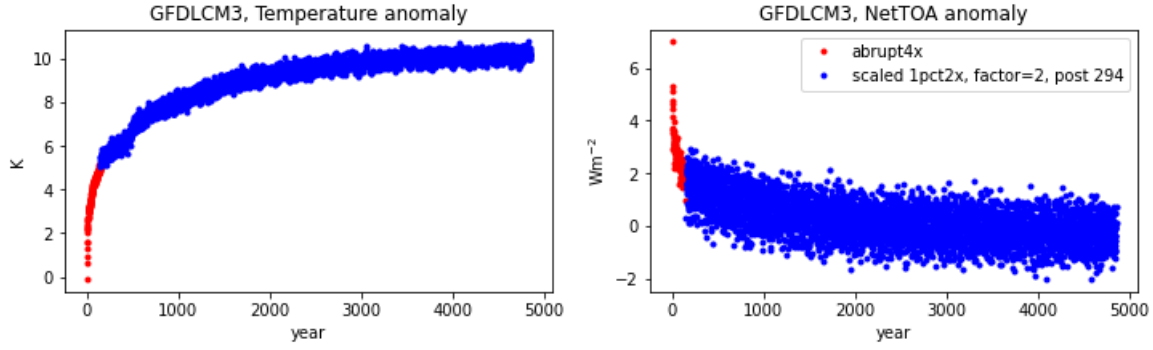

Figure A2. Illustration of composite *ABRUPT4X*CO_2 simulation for GFDLCM3

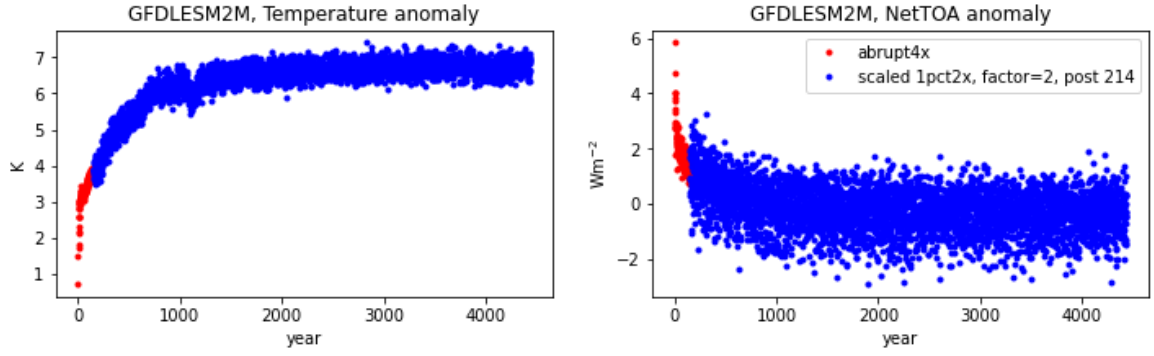

Figure A3. Illustration of composite *ABRUPT4X*CO_2 simulation for GFDLESM2M

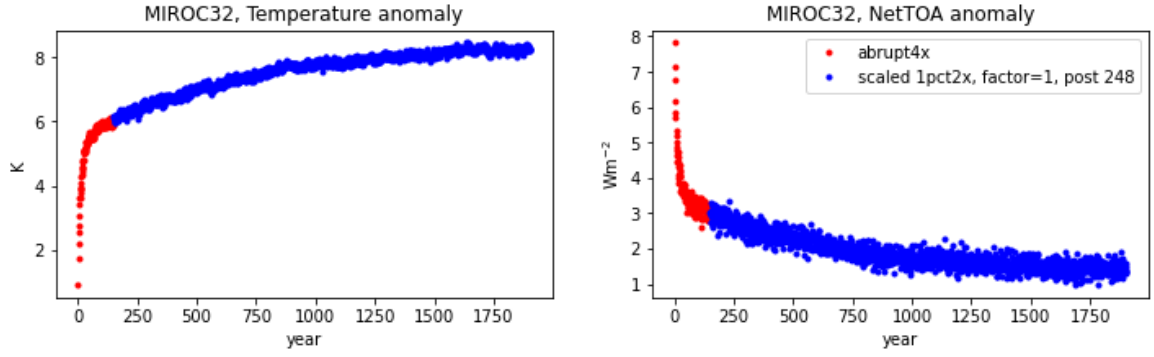

Figure A4. Illustration of composite *ABRUPT4X*CO_2 simulation for MIROC3.2

https://doi.org/10.5194/egusphere-2022-167
Preprint. Discussion started: 19 April 2022

Table A1. Table showing how models lacking multi-millennial *ABRUPT4X*CO_2 simulations were merged with other available simulations to create estimated long term *ABRUPT4X*CO_2 response

	Control Years	Abrupt 4X years	Spliced run	Spliced run length	Scaling Factor	Splice Year
CCSM3II	3805	3132				
CCSM3	1530	2120				
CESM104	1000	5900				
CNRMCM61	2000	1850				
ECEARTH	508	150	RCP8.5	1271	0.592	2258
ECHAM5MPIOM	100	1001				
FAMOUS	3000	3000				
GFDLCM3	5200	150	1pct2x	5000	2	294
GFDLESM2M	1340	150	1pct2x	4500	2	214
GISSE2R	5525	5001				
HadCM3L	1000	1000				
HadGEM2	239	1299				
IPSLCM5A	1000	1000				
MIROC32	681	150	1pct4x	2002	1	248
MPIESM11	2000	4459				

Model	Years	$EffCS$	$\Delta T_{best-est}$	ΔT_{extrap}	ζ_{LG}	ζ_{extrap}	R^{4x}_{extrap}	R^{CTRL}_0
CCSM3	2120	2.68	2.73	2.56 (2.55,2.55)	1.02	0.96 (0.95,0.95)	0.08 (0.07,0.09)	-0.04*
CESM104	5900	3.37	3.39	3.35 (3.35,3.35)	1.01	1.0 (0.99,0.99)	0.02 (0.01,0.03)	-0.02*
CNRMCM61	1850	5.42	5.51	4.48 (4.47,4.47)	1.02	0.83 (0.83,0.83)	1.26 (1.25,1.27)	0.73*
ECEARTH	1168	3.55	3.55	3.86 (3.82,3.82)	1.00	1.09 (1.08,1.08)	-0.21 (-0.26,-0.19)	-0.06*
ECHAM5MPIOM	1001	5.84	5.81	5.44 (5.37,5.37)	0.99	0.93 (0.92,0.92)	0.75 (0.25,1.04)	0.92
FAMOUS	3000	7.13	9.27	6.87 (6.86,6.86)	1.30	0.96 (0.96,0.96)	0.13 (0.07,0.14)	0.03*
GFDLCM3	4856	4.68	4.72	5.01 (5.0,5.0)	1.01	1.07 (1.07,1.07)	-0.16 (-0.18,-0.14)	-0.01*
GFDLESM2M	4436	3.19	3.24	3.34 (3.33,3.33)	1.01	1.05 (1.04,1.04)	-0.13 (-0.14,-0.12)	-0.05*
GISSE2R	5001	2.40	2.42	2.4 (2.4,2.4)	1.01	1.0 (1.0,1.0)	0.05 (0.05,0.06)	0.04
HadCM3L	1000	3.28	3.48	3.03 (2.99,2.99)	1.06	0.92 (0.91,0.91)	0.26 (0.03,0.39)	0.10
HadGEM2	1299	4.69	4.77	4.56 (4.46,4.46)	1.02	0.97 (0.95,0.95)	0.32 (0.12,0.43)	0.19
IPSLCM5A	1000	4.33	4.80	3.72 (3.7,3.7)	1.11	0.86 (0.85,0.85)	0.38 (0.19,0.51)	0.12*
MIROC32	1904	4.41	4.49	4.24 (4.23,4.23)	1.02	0.96 (0.96,0.96)	0.66 (0.65,0.68)	0.49*
MPIESM11	4459	3.42	3.42	3.46 (3.45,3.45)	1.00	1.01 (1.01,1.01)	0.23 (0.22,0.24)	0.24
MPIESM12	1000	3.35	3.34	3.33 (3.2,3.2)	1.00	0.99 (0.95,0.95)	0.17 (-0.18,0.37)	0.24

Table A2. Fitted parameters and uncertainties for the LongrunMIP experiments. Median values, with 5th and 95th percentiles in brackets where relevant. * indicate cases where R^{CTRL}_0 lies outside the 5-95th percentiles of R^{4x}_{extrap}.

https://doi.org/10.5194/egusphere-2022-167
Preprint. Discussion started: 19 April 2022

Model	Years	$EffCS$	$\Delta T_{best-est}$	ΔT_{extrap}	ζ_{LG}	ζ_{extrap}	R^{4x}_{extrap}	R_0^{CTRL}
ACCESS1-0	150	3.87	-	5.91 (3.73,3.73)	-	1.52 (0.96,0.96)	-0.08 (-1.74,0.87)	0.31
ACCESS1-3	151	3.54	-	4.88 (3.04,3.04)	-	1.38 (0.86,0.86)	-0.07 (-1.55,0.89)	0.13
CCSM4	104	3.98	-	3.43 (2.58,2.58)	-	0.86 (0.65,0.65)	0.68 (-1.36,1.84)	-0.01
CNRM-CM5	150	3.26	-	5.51 (3.41,3.41)	-	1.69 (1.05,1.05)	0.45 (-1.22,1.93)	1.84
CSIRO-Mk3-6-0	150	4.15	-	6.26 (3.93,3.93)	-	1.51 (0.95,0.95)	-0.15 (-1.76,0.89)	0.33
CanESM2	5	-	-	5.75 (3.72,3.72)	-	nan (nan,nan)	-1.22 (-2.27,0.43)	0.11
FGOALS-s2	150	4.23	-	6.06 (4.09,4.09)	-	1.43 (0.97,0.97)	-0.37 (-1.95,1.09)	0.47
GFDL-CM3	150	3.94	-	4.81 (3.32,3.32)	-	1.22 (0.84,0.84)	-0.56 (-2.01,0.56)	0.18
GFDL-ESM2G	300	2.57	-	3.77 (2.79,2.79)	-	1.47 (1.09,1.09)	-0.91 (-1.94,-0.0)	-0.01
GFDL-ESM2M	300	2.68	-	5.15 (3.7,3.7)	-	1.92 (1.38,1.38)	-0.44 (-1.68,0.29)	0.02
GISS-E2-H	151	2.43	-	4.85 (3.24,3.24)	-	1.99 (1.33,1.33)	-1.39 (-2.28,-0.02)	0.54
GISS-E2-R	151	2.36	-	4.71 (2.7,2.7)	-	2.0 (1.15,1.15)	-0.69 (-2.03,0.47)	0.13
HadGEM2-ES	5	-	-	5.64 (3.8,3.8)	-	nan (nan,nan)	-1.19 (-2.26,0.42)	0.20
IPSL-CM5A-LR	5	-	-	4.81 (3.53,3.53)	-	nan (nan,nan)	-1.01 (-2.22,0.69)	0.17
IPSL-CM5A-MR	140	4.10	-	5.84 (3.39,3.39)	-	1.43 (0.83,0.83)	0.21 (-1.3,1.04)	0.22
IPSL-CM5B-LR	160	2.63	-	4.21 (2.55,2.55)	-	1.61 (0.97,0.97)	-0.72 (-2.05,0.29)	0.14
MIROC-ESM	150	4.65	-	6.47 (4.56,4.56)	-	1.39 (0.98,0.98)	-1.88 (-2.39,-0.97)	-1.41
MIROC5	6	-	-	3.27 (2.44,2.44)	-	nan (nan,nan)	-0.99 (-2.21,0.75)	-0.37
MPI-ESM-LR	150	3.63	-	5.8 (3.55,3.55)	-	1.6 (0.98,0.98)	-0.89 (-2.13,0.52)	0.27
MPI-ESM-P	150	3.45	-	5.84 (3.36,3.36)	-	1.69 (0.97,0.97)	-0.8 (-2.14,0.64)	0.28
NorESM1-M	150	2.80	-	4.87 (2.74,2.74)	-	1.74 (0.98,0.98)	0.53 (-1.21,1.6)	1.12
bcc-csm1-1-m	150	2.82	-	5.31 (3.23,3.23)	-	1.88 (1.15,1.15)	-1.28 (-2.27,-0.22)	-0.35
inmcm4	150	2.04	-	2.32 (1.73,1.73)	-	1.14 (0.85,0.85)	-0.06 (-1.25,0.81)	0.36

Table A3. Fitted parameters and uncertainties for the CMIP5 experiments

https://doi.org/10.5194/egusphere-2022-167
Preprint. Discussion started: 19 April 2022

Model	Years	$EffCS$	$\Delta T_{best-est}$	ΔT_{extrap}	ζ_{LG}	ζ_{extrap}	R^{4x}_{extrap}	R_0^{CTRL}
ACCESS-CM2	150	4.70	-	4.08 (3.43,3.43)	-	0.87 (0.73,0.73)	-0.52 (-2.07,0.86)	0.25
ACCESS-ESM1-5	150	3.86	-	6.25 (4.2,4.2)	-	1.62 (1.09,1.09)	-0.88 (-2.1,0.37)	-0.04
AWI-CM-1-1-MR	151	3.13	-	5.23 (3.11,3.11)	-	1.67 (0.99,0.99)	-0.86 (-2.17,0.4)	0.20
BCC-CSM2-MR	151	2.98	-	5.25 (3.03,3.03)	-	1.76 (1.02,1.02)	-0.95 (-2.17,-0.0)	-0.21
CAMS-CSM1-0	150	2.30	-	5.06 (2.77,2.77)	-	2.2 (1.2,1.2)	-0.58 (-2.03,0.62)	0.59
CESM2	400	6.08	-	7.38 (6.28,6.28)	-	1.21 (1.03,1.03)	-0.32 (-1.33,0.54)	0.41
CESM2-WACCM	150	4.71	-	7.21 (5.72,5.72)	-	1.53 (1.21,1.21)	-0.6 (-2.11,0.66)	0.10
CIESM	150	5.65	-	7.62 (4.99,4.99)	-	1.35 (0.88,0.88)	1.53 (-0.02,2.13)	1.19
CMCC-CM2-SR5	165	3.59	-	6.18 (4.1,4.1)	-	1.72 (1.14,1.14)	-0.14 (-1.82,1.39)	1.15
CNRM-CM6-1	150	4.90	-	6.56 (4.53,4.53)	-	1.34 (0.93,0.93)	-0.07 (-1.97,1.47)	0.78
CNRM-CM6-1-HR	150	4.38	-	6.72 (4.88,4.88)	-	1.53 (1.12,1.12)	-1.0 (-2.18,0.83)	0.88
CNRM-ESM2-1	150	4.72	-	4.07 (3.28,3.28)	-	0.86 (0.7,0.7)	-1.14 (-2.25,0.51)	0.79
CanESM5	151	5.65	-	7.49 (5.54,5.54)	-	1.33 (0.98,0.98)	-0.43 (-2.0,0.78)	0.11
EC-Earth3	160	4.37	-	6.98 (5.08,5.08)	-	1.6 (1.16,1.16)	-0.02 (-1.41,0.52)	0.09
FGOALS-f3-L	160	3.04	-	4.76 (3.06,3.06)	-	1.57 (1.01,1.01)	-0.81 (-2.15,0.46)	0.20
FGOALS-g3	152	2.87	-	4.02 (2.64,2.64)	-	1.4 (0.92,0.92)	-0.46 (-1.91,1.09)	0.99
GFDL-ESM4	150	2.66	-	4.05 (2.47,2.47)	-	1.52 (0.93,0.93)	-0.37 (-1.81,0.59)	0.12
GISS-E2-1-G	151	2.72	-	5.61 (3.86,3.86)	-	2.06 (1.42,1.42)	-0.81 (-2.1,0.5)	0.09
HadGEM3-GC31-LL	150	5.56	-	7.36 (5.04,5.04)	-	1.32 (0.91,0.91)	-0.27 (-1.92,0.84)	0.15
HadGEM3-GC31-MM	150	5.47	-	7.3 (5.91,5.91)	-	1.33 (1.08,1.08)	-0.79 (-2.14,0.69)	0.20
IITM-ESM	165	2.38	-	3.43 (2.2,2.2)	-	1.44 (0.93,0.93)	-0.14 (-1.7,0.95)	0.44
INM-CM4-8	150	1.83	-	4.47 (2.16,2.16)	-	2.44 (1.18,1.18)	0.28 (-1.42,1.76)	2.17
INM-CM5-0	150	1.91	-	4.33 (2.32,2.32)	-	2.27 (1.21,1.21)	-0.24 (-1.73,0.86)	0.88
KACE-1-0-G	151	4.70	-	6.13 (4.23,4.23)	-	1.3 (0.9,0.9)	0.42 (-1.45,1.43)	0.52
MIROC-ES2L	150	2.66	-	3.0 (2.24,2.24)	-	1.13 (0.84,0.84)	0.06 (-1.64,1.14)	0.48
MIROC6	250	2.62	-	3.79 (2.63,2.63)	-	1.45 (1.01,1.01)	0.38 (-0.8,1.15)	0.60
MPI-ESM1-2-HR	165	2.97	-	4.61 (3.01,3.01)	-	1.55 (1.01,1.01)	-0.96 (-2.17,0.29)	0.16
MPI-ESM1-2-LR	165	3.04	-	5.22 (2.85,2.85)	-	1.72 (0.94,0.94)	-1.29 (-2.26,0.28)	0.26
NESM3	150	4.64	-	6.77 (4.7,4.7)	-	1.46 (1.01,1.01)	-0.48 (-1.9,0.57)	-0.02
NorESM2-MM	150	2.43	-	4.38 (2.61,2.61)	-	1.8 (1.07,1.07)	-0.53 (-1.9,0.48)	0.05
TaiESM1	150	4.36	-	6.73 (4.65,4.65)	-	1.54 (1.07,1.07)	-0.77 (-2.13,0.61)	0.08
UKESM1-0-LL	150	5.37	-	6.82 (4.8,4.8)	-	1.27 (0.89,0.89)	-0.06 (-1.8,0.78)	0.05

Table A4. Fitted parameters and uncertainties for the CMIP6 experiments

Code and data availability. All code to reproduce this study is available at https://doi.org/10.5281/zenodo.6424714. CMIP5 and CMIP6 source data is freely available, and was here accessed on the Google Public Cloud https://console.cloud.google.com/storage/browser/cmip6. Longrunmip data is available on request at http://www.longrunmip.org/

Author contributions. BMS performed all calculations, produced plots and wrote main text. MR produced ESM data and co-wrote main text.

Competing interests. The authors have no competing interests

References

Andrews, T., Gregory, J. M., Webb, M. J., and Taylor, K. E.: Forcing, feedbacks and climate sensitivity in CMIP5 coupled atmosphere-ocean climate models, Geophysical research letters, 39, 2012.

Andrews, T., Gregory, J. M., and Webb, M. J.: The dependence of radiative forcing and feedback on evolving patterns of surface temperature change in climate models, Journal of Climate, 28, 1630–1648, 2015.

Andrews, T., Gregory, J. M., Paynter, D., Silvers, L. G., Zhou, C., Mauritsen, T., Webb, M. J., Armour, K. C., Forster, P. M., and Titchner, H.: Accounting for Changing Temperature Patterns Increases Historical Estimates of Climate Sensitivity, Geophys. Res. Lett., 45, 8490–8499, https://doi.org/10.1029/2018GL078887, 2018.

https://doi.org/10.5194/egusphere-2022-167
Preprint. Discussion started: 19 April 2022

Armour, K. C., Bitz, C. M., and Roe, G. H.: Time-Varying Climate Sensitivity from Regional Feedbacks, J. Clim., 26, 4518–4534, https://doi.org/10.1175/JCLI-D-12-00544.1, 2013.

Bloch-Johnson, J., Rugenstein, M., Stolpe, M. B., Rohrschneider, T., Zheng, Y., and Gregory, J. M.: Climate sensitivity increases under higher CO2 levels due to feedback temperature dependence, Geophysical Research Letters, 48, e2020GL089 074, 2021.

Caldeira, K. and Myhrvold, N. P.: Projections of the pace of warming following an abrupt increase in atmospheric carbon dioxide concentration, Environ. Res. Lett., 8, 034 039, https://doi.org/10.1088/1748-9326/8/3/034039, 2013.

Charney, J. G., Arakawa, A., Baker, D. J., Bolin, B., Dickinson, R. E., Goody, R. M., Leith, C. E., Stommel, H. M., and Wunsch, C. I.: Carbon dioxide and climate: a scientific assessment, National Academy of Sciences, Washington, DC, https://doi.org/10.17226/12181, 1979.

Dunne, J. P., Winton, M., Bacmeister, J., Danabasoglu, G., Gettelman, A., Golaz, J.-C., Hannay, C., Schmidt, G. A., Krasting, J. P., Leung, L. R., et al.: Comparison of equilibrium climate sensitivity estimates from slab ocean, 150-year, and longer simulations, Geophysical Research Letters, 47, e2020GL088 852, 2020.

Eyring, V., Bony, S., Meehl, G. A., Senior, C. A., Stevens, B., Stouffer, R. J., and Taylor, K. E.: Overview of the Coupled Model Intercomparison Project Phase 6 (CMIP6) experimental design and organization, Geosci. Model Dev., 9, 1937–1958, https://doi.org/10.5194/gmd-9-1937-2016, 2016.

Foreman-Mackey, D., Hogg, D. W., Lang, D., and Goodman, J.: emcee: The MCMC Hammer, Publ. Astron. Soc. Pac., 125, 306–312, https://doi.org/10.1086/670067, 2013.

Forster, P. M.: Inference of climate sensitivity from analysis of Earth's energy budget, Annual Review of Earth and Planetary Sciences, 44, 85–106, 2016.

Geoffroy, O., Saint-Martin, D., Bellon, G., Voldoire, A., Olivié, D. J. L., and Tytéca, S.: Transient Climate Response in a Two-Layer Energy-Balance Model. Part II: Representation of the Efficacy of Deep-Ocean Heat Uptake and Validation for CMIP5 AOGCMs, J. Clim., 26, 1859–1876, https://doi.org/10.1175/JCLI-D-12-00196.1, 2013a.

Geoffroy, O., Saint-Martin, D., Olivié, D. J. L., Voldoire, A., Bellon, G., and Tytéca, S.: Transient Climate Response in a Two-Layer Energy-Balance Model. Part I: Analytical Solution and Parameter Calibration Using CMIP5 AOGCM Experiments, J. Clim., 26, 1841–1857, https://doi.org/10.1175/JCLI-D-12-00195.1, 2013b.

Gregory, J. M., Ingram, W. J., Palmer, M. A., Jones, G. S., Stott, P. A., Thorpe, R. B., Lowe, J. A., Johns, T. C., and Williams, K. D.: A new method for diagnosing radiative forcing and climate sensitivity, Geophys. Res. Lett., 31, https://doi.org/10.1029/2003GL018747, 2004.

Hansen, J., Lacis, A., Rind, D., Russell, G., Stone, P., Fung, I., Ruedy, R., and Lerner, J.: Climate sensitivity: Analysis of feedback mechanisms., feedback, 1, 1–3, 1984.

Hobbs, W., Palmer, M. D., and Monselesan, D.: An energy conservation analysis of ocean drift in the CMIP5 global coupled models, Journal of Climate, 29, 1639–1653, 2016.

IPCC: Climate Change 2013: The Physical Science Basis. Contribution of Working Group I to the Fifth Assessment Report of the Intergovernmental Panel on Climate Change, Cambridge University Press, Cambridge, United Kingdom and New York, NY, USA, https://doi.org/10.1017/CBO9781107415324, 2013.

Irving, D., Hobbs, W., Church, J., and Zika, J.: A mass and energy conservation analysis of drift in the CMIP6 ensemble, Journal of Climate, 34, 3157–3170, 2021.

Jarvis, A. and Li, S.: The contribution of timescales to the temperature response of climate models, Climate dynamics, 36, 523–531, 2011.

Jiménez-de-la Cuesta, D. and Mauritsen, T.: Emergent constraints on Earth's transient and equilibrium response to doubled CO2 from post-1970s global warming, Nature Geoscience, 12, 902–905, 2019.

Knutti, R., Rugenstein, M. A. A., and Hegerl, G. C.: Beyond equilibrium climate sensitivity, Nat. Geosci., 10, 727–736, https://doi.org/10.1038/ngeo3017, 2017.

Masson-Delmotte, V., Zhai, P., Pirani, A., Connors, S., Péan, C., Berger, S., Caud, N., Chen, Y., Goldfarb, L., Gomis, M., Huang, M., Leitzell, K., Lonnoy, E., Matthews, J., Maycock, T., Waterfield, T., Yelekçi, O., Yu, R., and Zhou, B.: Climate Change 2021: The Physical Science Basis. Contribution of Working Group I to the Sixth Assessment Report of the Intergovernmental Panel on Climate Change, Cambridge University Press, Cambridge, United Kingdom and New York, NY, USA, https://www.ipcc.ch/assessment-report/ar6/, 2021.

Meehl, G. A., Senior, C. A., Eyring, V., Flato, G., Lamarque, J.-F., Stouffer, R. J., Taylor, K. E., and Schlund, M.: Context for interpreting equilibrium climate sensitivity and transient climate response from the CMIP6 Earth system models, Science Advances, 6, eaba1981, 2020.

Meinshausen, M., Smith, S. J., Calvin, K., Daniel, J. S., Kainuma, M. L. T., Lamarque, J.-F., Matsumoto, K., Montzka, S. A., Raper, S. C. B., Riahi, K., Thomson, A., Velders, G. J. M., and van Vuuren, D. P. P.: The RCP greenhouse gas concentrations and their extensions from 1765 to 2300, Clim. Change, 109, 213–241, https://doi.org/10.1007/s10584-011-0156-z, 2011.

Murphy, J.: Transient response of the Hadley centre coupled ocean-atmosphere model to increasing carbon dioxide. Part 1: control climate and flux adjustment, Journal of Climate, 8, 36–56, 1995.

Myhre, G., Shindell, D., Bréon, F., Collins, W., Fuglestvedt, J., Huang, J., Koch, D., Lamarque, J., Lee, D., Mendoza, B., et al.: Anthropogenic and natural radiative forcing, Climate change 2013: The physical science basis. Contribution of working group I to the fifth assessment report of the Intergovernmental Panel on Climate Change, pp. 659–740, 2013.

Nijsse, F. J., Cox, P. M., and Williamson, M. S.: Emergent constraints on transient climate response (TCR) and equilibrium climate sensitivity (ECS) from historical warming in CMIP5 and CMIP6 models, Earth System Dynamics, 11, 737–750, 2020.

O'Neill, B. C., Tebaldi, C., Vuuren, D. P. v., Eyring, V., Friedlingstein, P., Hurtt, G., Knutti, R., Kriegler, E., Lamarque, J.-F., Lowe, J., et al.: The scenario model intercomparison project (ScenarioMIP) for CMIP6, Geoscientific Model Development, 9, 3461–3482, 2016.

https://doi.org/10.5194/egusphere-2022-167
Preprint. Discussion started: 19 April 2022

Pfister, P. L. and Stocker, T. F.: State-Dependence of the Climate Sensitivity in Earth System Models of Intermediate Complexity, Geophysical Research Letters, 44, 10–643, 2017.

Proistosescu, C. and Huybers, P. J.: Slow climate mode reconciles historical and model-based estimates of climate sensitivity, Sci. Adv., 3, e1602 821, https://doi.org/10.1126/sciadv.1602821, 2017.

Rugenstein, M., Bloch-Johnson, J., Abe-Ouchi, A., Andrews, T., Beyerle, U., Cao, L., Chadha, T., Danabasoglu, G., Dufresne, J.-L., Duan, L., et al.: LongRunMIP: motivation and design for a large collection of millennial-length AOGCM simulations, Bulletin of the American Meteorological Society, 100, 2551–2570, 2019.

Rugenstein, M., Bloch-Johnson, J., Gregory, J., Andrews, T., Mauritsen, T., Li, C., Frölicher, T. L., Paynter, D., Danabasoglu, G., Yang, S., et al.: Equilibrium climate sensitivity estimated by equilibrating climate models, Geophysical Research Letters, 47, e2019GL083 898, 2020.

Rugenstein, M. A. and Armour, K. C.: Three flavors of radiative feedbacks and their implications for estimating Equilibrium Climate Sensitivity, Geophysical Research Letters, 48, e2021GL092 983, 2021.

Rugenstein, M. A. A., Caldeira, K., and Knutti, R.: Dependence of global radiative feedbacks on evolving patterns of surface heat fluxes, Geophys. Res. Lett., 43, 9877–9885, https://doi.org/10.1002/2016GL070907, 2016.

Sanderson, B.: Relating climate sensitivity indices to projection uncertainty, Earth System Dynamics, 11, 721–735, 2020.

Senior, C. A. and Mitchell, J. F. B.: The time-dependence of climate sensitivity, Geophys. Res. Lett., 27, 2685–2688, https://doi.org/10.1029/2000GL011373, 2000.

Sherwood, S., Webb, M. J., Annan, J. D., Armour, K., Forster, P. M., Hargreaves, J. C., Hegerl, G., Klein, S. A., Marvel, K. D., Rohling, E. J., et al.: An assessment of Earth's climate sensitivity using multiple lines of evidence, Reviews of Geophysics, 58, e2019RG000 678, 2020.

Smith, C. J., Forster, P. M., Allen, M., Leach, N., Millar, R. J., Passerello, G. A., and Regayre, L. A.: FAIR v1.3: a simple emissions-based impulse response and carbon cycle model, Geosci. Model Dev., 11, 2273–2297, https://doi.org/10.5194/gmd-11-2273-2018, 2018.

Solomon, S., Daniel, J. S., Sanford, T. J., Murphy, D. M., Plattner, G.-K., Knutti, R., and Friedlingstein, P.: Persistence of climate changes due to a range of greenhouse gases, Proceedings of the National Academy of Sciences, 107, 18 354–18 359, 2010.

Taylor, K. E., Stouffer, R. J., and Meehl, G. A.: An overview of CMIP5 and the experiment design, Bulletin of the American meteorological Society, 93, 485–498, 2012.

Tokarska, K. B. and Gillett, N. P.: Cumulative carbon emissions budgets consistent with 1.5 °C global warming, Nat. Clim. Change, 8, 296–299, https://doi.org/10.1038/s41558-018-0118-9, 2018.

Tokarska, K. B., Stolpe, M. B., Sippel, S., Fischer, E. M., Smith, C. J., Lehner, F., and Knutti, R.: Past warming trend constrains future warming in CMIP6 models, Science advances, 6, eaaz9549, 2020.

Wetherald, R. T., Stouffer, R. J., and Dixon, K. W.: Committed warming and its implications for climate change, Geophysical Research Letters, 28, 1535–1538, 2001.

Winton, M., Takahashi, K., and Held, I. M.: Importance of ocean heat uptake efficacy to transient climate change, Journal of Climate, 23, 2333–2344, 2010.

Zelinka, M. D., Myers, T. A., McCoy, D. T., Po-Chedley, S., Caldwell, P. M., Ceppi, P., Klein, S. A., and Taylor, K. E.: Causes of higher climate sensitivity in CMIP6 models, Geophysical Research Letters, 47, e2019GL085 782, 2020.

Zhu, J., Poulsen, C. J., and Otto-Bliesner, B. L.: High climate sensitivity in CMIP6 model not supported by paleoclimate, Nature Climate Change, 10, 378–379, 2020.